Supporting Information

Soriano *et al.* 10.1073/pnas.0707492105

SI Text

The supporting information includes three main parts. First, we provide details on the experimental procedure, on the characterization of the connectivity probability between neurons, and a table with the range of variation of g_{syn}. We then extend the experimental results and describe the measurements of spontaneous activity during development. Finally, we introduce our percolation model and derive the relation between the critical points $m_E = m'_c m_0$ and $m_{EI} = m_c m_0$ with the average number of excitatory and inhibitory inputs, $\bar{k}_E$ and $\bar{k}_I$, respectively. We show that they are related through $m_E = 0.8\bar{k}_E$, and $m_{EI} \simeq \bar{k}_E - \bar{k}_I$. By using these results, we show that the ratio between excitation and inhibition in the network is given by $\bar{k}_I/\bar{k}_E \simeq 1 - m_{EI}/m_E$.

Methods

Neural Cultures. Primary cultures of rat hippocampal and cortical neurons were prepared following the procedure described by Papa *et al.* (1). Embryonic brains with either 17 (E17) or 19 (E19) days of development, and postnatal brains just after birth (P0) were dissected from Wistar rats, and neurons were dissociated by mechanical trituration. Dissociated neurons were plated onto 13-mm glass cover slips (#1 Menzel–Glaser) coated with poly-L-lysine, with nominal densities in the range $1.3 - 21 \times 10^3$ neurons per mm^2. Cultures were incubated at 37°C, 5% CO_2 for 3 days in plating medium [90% Eagle's MEM, supplemented with 0.6% glucose, 1% 100× glutamax (Gibco), and 20 μg/ml gentamicin, with 5% heat-inactivated horse serum, 5% heat-inactivated FCS, and 1 μl/ml B27]. The medium was next switched to changing medium [90% supplemented MEM, 9.5% heat-inactivated horse serum, and 0.5% FUDR (5-fluorodeoxyuridine)] for 3 days to limit glia growth, and thereafter to final medium (90% supplemented MEM and 10% heat-inactivated horse serum). The final medium was refreshed every 3 days by replacing one-third of the culture well volume. Examples of hippocampal and cortical cultures are shown in Fig. S1.

Different Densities. Different densities were obtained by varying the nominal density ρ_n in the range $1.3–21 \times 10^3$ neurons per mm^2 (Fig. S2). The actual density ρ was measured at the end of each experiment by counting the number of active neurons in a region of the culture, and averaging over different regions. Cultures corresponding to the same batch (dissection) provided similar final densities, with fluctuations <10%. Cultures derived from different dissections with identical nominal density showed strong variations in the final density, between 50% and 200%.

Low nominal densities ($\rho_n \lesssim 1{,}300$ neurons per mm^2 for hippocampal cultures, and $\rho_n \lesssim 4{,}000$ neurons per mm^2 for cortical) did not produce a network in 90% of the cases. This made the study of very sparse networks difficult. The final density ρ increased in proportion to ρ_n for intermediate nominal densities, but large nominal densities $\rho_n \gtrsim 10^4$ neurons per mm^2 provided the same final density, ≈1,000 neurons per mm^2, so that it was not possible to obtain arbitrarily highly dense networks. Hence, our exploration of densities was limited between 150 and 1,100 neurons per mm^2.

In our experiments we have obtained a maximum density of ≈1,000 neurons per mm^2. Wagenaar *et al.* (2) reported highly dense cultures to have ≈2,500 neurons per mm^2, which is similar to our cultures. Therefore, in general, it seems difficult to obtain a highly dense, monolayered neuronal culture. Perfectly packed cells would give rise to a density of ≈10^4 neurons per mm^2, which is one order of magnitude higher than a typical dense culture and is clearly unreachable in our cultures.

Experimental Procedures

To characterize the disintegration of the network as a function of the concentration of CNQX we always used mature cultures, at day *in vitro* (DIV) 14–21. We observed little or no variance in the response of the network for cultures studied in this range of ages. Since cultures start to degrade by DIV 25–30, we did not use cultures older than 21 days in our experiments.

Cultures were carefully inspected visually before use, and those with strong fluctuations in density or consisting of highly dense aggregates of cells were rejected. With standard culturing conditions, no more than 10% of the cultures were rejected. Before imaging, cultures were incubated for 60 min in external medium (128 mM NaCl, 1 mM $CaCl_2$, 1 mM $MgCl_2$, 45 mM sucrose, 10 mM glucose, and 0.01 M Hepes, pH 7.4) in the presence of the cell-permeant, calcium-sensitive dye Fluo-4-AM (2 μl Fluo-4 per ml of external medium.) The culture was then washed with fresh external medium and placed for study in the chamber equipped with bath electrodes.

To monitor the network's response we first randomly selected an initial set of 100 individual neurons and recorded their spontaneous activity for 3 min. We next measured the response of the neurons to the external excitation for a given concentration of CNQX and increasing voltages. Each measurement consisted of 30 sec of recording at a rate of five images per second, with the excitation typically applied during the first 10 s. Neurons were left unperturbed for 1–3 min between measurements. The resting time depended on the strength of the response to the excitation. In general, we observed that 2 min was sufficient to prevent an increased sensitivity of the neurons because of repeated excitation. We also carried out control experiments where we measured the response of the network with increasing voltages and next with decreasing voltages. We measured the same response curve with a maximum variation of ≈5%.

Each response curve was completed within 10–15 min. The next concentration of CNQX was then applied, and the culture was left unperturbed and in darkness for ≈10 min for the drug to take effect. The entire experiment (8–10 response curves) was completed in ≈4–5 h.

At the end of the experiment the images were analyzed in detail to include all neurons available in the field of view and to reject glial cells and dead neurons. The final response curves were based on the statistics of 100 neurons for the lowest density, and of 900 for the highest.

We carried out control experiments to check the importance of fluctuations in density in our results. We measured, for instance, a number of response curves for the same concentration of CNQX and at different locations of the neural culture. We observed a very similar behavior from region to region, with fluctuations in the size of the giant component of ≈5%. In general, the variation in the response curves from region to region of the same culture was much smaller than the variation between cultures of different densities. We also observed that cultures of the same batch and with identical nominal densities gave rise to very similar response curves.

In our experiments we study the role of inhibition by blocking the $GABA_A$ receptors of inhibitory synapses with the antagonist bicuculine. The blocking of $GABA_B$ receptors has a minor effect on neurons' excitability (3), and therefore, we left $GABA_B$

active. However, we carried out control experiments to verify that additional blocking of $GABA_B$ with either 5 μM CGP-55845 or 100 μM saclofen did not change the response of the network within experimental error. Hence, application of APV, CNQX, and bicuculine was sufficient to completely disrupt the synaptic connections.

Precise Determination of the Control Parameter. After *Characterization of the Control Parameter* in *Materials and Methods*, the synaptic strength between neurons can be quantified by the fraction c of receptor molecules that are not bound to the antagonist CNQX and are therefore free to activate the synapse. This fraction is given by $c = 1/(1 + [\mathrm{CNQX}]/K_d)$, where the dissociation constant K_d is the concentration of CNQX at which 50% of the receptors are blocked (4). c takes values between 0 (full blocking) and 1 (full connectivity).

The relation between c and [CNQX] was verified by using two antagonists with different dissociation constants K_d, CNQX (K_d = 300 nM) and DNQX (K_d = 500 nM). As shown in Fig. S3*A*, the giant component grows similarly with either [CNQX] or [DNQX], but the curves are shifted horizontally because of the different affinities of the receptors. The two curves collapse when plotted as a function of the parameter c, as shown in Fig. S3*B*, indicating that c is the appropriate variable to describe the fraction of free receptors in the synapse.

Range of Variation of the Synaptic Voltage g_{syn}. We study the disintegration of the network in terms of a single control parameter $m = V_T/g_{syn}$ that quantifies the average number of inputs needed to activate a neuron. In terms of the concentration of CNQX, the order parameter takes the form $m = m_0\ (1 + [\mathrm{CNQX}]/K_d)$, with K_d = 300 nM and m_0 the number of inputs required for a neuron to fire in the unperturbed network.

In our percolation approach we use the value of the order parameter m at transition to determine the average number of input connections per neuron. The average connectivity that we measure is therefore sensitive to the value of m_0 chosen, which in turn depends on the values of V_T and g_{syn}. A literature survey provides $V_T \simeq 30$ mV. A precise value of g_{syn}, however, seems difficult and varies from source to source. We provide in Table S1 a summary of the different values of g_{syn} and the corresponding values of m_0. Experimentally we are not sensitive to the large variance in g_{syn} because we average over many neuronal inputs in the network. The average value of g_{syn} is much more stable, and we use for it the approximate value of 2 mV, which is compatible with the results of Thomson *et al.* (7). We therefore use $m_0 = 15$ in the analysis of our experimental results.

Spontaneous Activity During Development. We investigated how the generation of spontaneous activity is related to the appearance of a giant connected component during development, and compared the behaviors of E17, E19, and P0 cultures. We identified a number of groups of neurons that tended to fire together simultaneously in a spontaneous manner (Fig. S4*A*). As a quantitative measure of the level of spontaneous activity in the culture we took the largest such fraction of neurons.

We first found that in the time interval during which neurons did not respond to the external excitation they were also not active in spontaneous bursting (DIV 0–1 for P0, DIV 0–2 for E19, and DIV 0–3 for E17). The appearance of synchronous activity coincided with the emergence of the giant component. At the beginning, the activity was scattered and restricted to small groups of neurons (Fig. S4*A Top*). The groups gradually grew, coalesced, and extended to cover larger areas of culture until finally the entire network fired in unison (Fig. S4*A Bottom*).

As shown in Fig. S4*B*, the largest fraction of neurons firing together in spontaneous activity increased at the same rate as the size of the giant component. For $g = 1$ (full connectivity of the network) the spontaneous activity extended to the entire culture. This occurs for neurons from different embryonic days, in all cases the occurrence of spontaneous activity extending the entire culture coincided with $g = 1$ (Fig. S4*C*).

We also observed that the time of emergence of full connectivity in the network, and therefore network bursting, can shift according to the density of the neural culture. In general, denser cultures develop faster, an observation that is supported by Wagenaar *et al.* (2), who studied bursting patterns in E18 cortical cultures and found that denser cultures exhibited bursting behavior earlier than sparser cultures.

The concurrence of spontaneous activity with the formation of the giant component seems natural. Similar results were also obtained by Kamioka *et al.* (10), who studied E17 cortical cultures and observed that partial synchronous bursting started at day 4, initially comprising a fraction of the network and then extending to the entire culture by day 5–6. Wagenaar *et al.* (2) observed that network bursting in E18 cortical cultures appeared at day 4–6, close to the expected time of birth. This agrees with our observation that the beginning of network bursting coincides with the formation of the giant component. It is reasonable to assume that spontaneous activity appears once long-range connectivity is established in the network, and extends across the culture as the fraction of connected neurons increases. The globally synchronous spontaneous activity emerges once global connectivity is established.

Percolation Model: Relation Between the Critical Points and the Average Connectivity. As described in *Giant Component, Connectivity and Amount of Inhibition in the Network* in *Materials and Methods*, the giant component g decreases with m, which is the minimal number of active inputs required for a neuron to fire. The giant component disintegrates at a critical value that depends on the average connectivity of the network and on the ratio between excitation and inhibition. m_{EI} denotes the critical point for networks containing both excitatory and inhibitory inputs, and m_E is the critical point with excitatory inputs only. We are interested in the relationship between m_{EI}, m_E, and the average number of excitatory and inhibitory inputs, $\bar{k}_E$ and $\bar{k}_I$, respectively. In particular, we want to show that $m_E \sim \bar{k}_E$ and that $m_{EI} \simeq \bar{k}_E - \bar{k}_I$.

In a previous work (11) we showed that percolation on a neural network can be described in terms of bond–percolation on a directed graph. Here, we consider a more elaborate model that takes into account that m inputs are required to excite a neuron (M.R.M., J.S., E.M., T.T., unpublished data). In the framework of this model, the neighboring upstream neurons that can excite a certain neuron define its input-cluster or excitation-basin. A neuron fires as a direct response to the externally applied electrical stimulus or if at least m neurons of its input-cluster fire. The model ignores the presence of feedback loops and recurrent activity in the neural culture. The model also assumes, for simplicity, that all neurons have at least m_0 inputs, that all inputs have the same weight or synaptic efficacy, and that all inputs reach the target neuron simultaneously.

Under these assumptions, the firing probability p of a neuron is the sum of the probability of being externally excited f, and the probability that at least m neurons of the input-cluster fire,

$$p = f + (1 - f)P\ (\text{at least } m \text{ input neurons fire})$$

$$= f + (1 - f) \sum_{k=m}^{\infty} p_k \sum_{l=m}^{k} \binom{k}{l} p^l\ (1 - p)^{k-l} \qquad [1]$$

where p_k is the degree distribution, that is, the probability for a neuron to have k input neurons, and the second sum counts the number of possibilities of chosing m neurons out of k.

Because the neural network contains both excitatory and inhibitory inputs, we consider two degree distributions, one for the excitatory inputs (with average connectivity $\bar{k}_E$) and another for the inhibitory one (average connectivity $\bar{k}_I$). The condition for a neuron to fire is that the number of excitatory inputs, e, *minus* the number of inhibitory inputs, i, is equal or larger than m,

$$p = f + (1 - f)P(e - i \geq m). \qquad [2]$$

We are interested in the relationship between $\bar{k}_E, \bar{k}_I, m_{EI}$, and m_E, and how this relationship depends on the degree distribution p_k. We assume that the excitatory and inhibitory subnetworks have the same degree distributions.

We consider two distributions, exponential and Poisson. The exponential distribution permits the derivation of analytic expressions for the relationship between the critical parameters. The Poisson distribution, on the other hand, is convenient because it contains a single parameter (the average connectivity) and is a good approximation of a Gaussian distribution, which describes realistically the connectivity in a cultured neural network (11).

Exponential Distribution. The exponential degree distribution is given by $p_k = \bar{k}^k/(1 + \bar{k})^{k+1}$, with $\bar{k}$ the average number of inputs per neuron. In a network with only excitation ($\bar{k} = \bar{k}_E$) the condition for critical percolation, that is, the critical value m_E at which the giant component emerges is obtained by solving Eq. **1** for the exponential distribution. After some straightforward but cumbersome algebra we obtain:

$$\bar{k}_E = \frac{m_E^{m_E}}{(m_E - 1)^{m_E - 1}}. \qquad [3]$$

For large m_E (which is the case in our experiments, with $m_E \simeq 40$) the above equation leads to $\bar{k}_E \simeq e\, m_E$.

When inhibition is present, the condition for critical percolation becomes

$$\left(\frac{\alpha - 2}{\alpha}\right)^{m_{E1} - 1} = \frac{2\bar{k}_E + (\alpha - 2)(\bar{k}_E + \bar{k}_I)}{2\bar{k}_E^2}, \qquad [4]$$

where

$$\alpha = m_{EI} + \sqrt{m_{EI}^2 - 4(m_{EI} - 1)\frac{\bar{k}_I}{\bar{k}_E + \bar{k}_I}}. \qquad [5]$$

Notice that when there is no inhibition, that is, $\bar{k}_I = 0$, then $\alpha = 2\, m_{EI}$ and Eq. **4** simplifies to Eq. **3**.

According to our experimental results the critical points m_E and m_{EI} are on the order of 30–90 (for $m_0 = 15$). Hence, we can perform in Eqs. **4** and **5** an expansion for high values of the critical points, leading to

$$m_{EI} \simeq \frac{m_E}{1 + \gamma} + \frac{\gamma^2 + 3\gamma - 1}{2(1 + \gamma)}, \qquad [6]$$

where $\gamma = \bar{k}_I/\bar{k}_E$. For real neural networks the number of excitatory inputs exceeds the number of inhibitory ones, with γ in the range 0.25–0.33. For these values, the second term of the right-hand side of Eq. **6** is negligible with respect to the first one, and thus

$$\frac{m_{EI}}{m_E} \simeq \frac{1}{1 + \gamma} \simeq 1 - \gamma. \qquad [7]$$

Therefore, the ratio between excitation and inhibition in the network is well approximated by $\bar{k}_I/\bar{k}_E \simeq 1 - m_{EI}/m_E$.

Poisson Distribution. Let us now consider a Poisson distribution with $\bar{k}$ average number of inputs and degree distribution given by $p_k = e^{-\bar{k}}\bar{k}^k/k$. In this case, the condition for critical percolation cannot be solved analytically and we therefore resort to numerical simulations.

Fig. S5 shows the dependence of $\bar{k}_E$ on the critical value of m for a Poisson distribution, and for gradually higher values of $\bar{k}_I$. For the case without inhibition, $\bar{k}_I = 0$, the average connectivity $\bar{k}_E$ increases linearly with the critical point m_E, with a slope ≈ 1.3. Hence, for the case without inhibition, $m_E \simeq \bar{k}_E$. When inhibition is introduced, $\bar{k}_E$ still varies linearly with m_{EI} and with a similar slope, but the curves shifts upward as $\bar{k}_I$ increases. The relative shift between curves is proportional to $\bar{k}_I$, and indicates that inhibition effectively reduces the average connectivity of the network. From the analysis of the data shown in Fig. S5 we obtain the following expression:

$$\frac{m_{EI}}{m_E} = \left(1 - 0.92\frac{\bar{k}_I}{\bar{k}_E}\right) - \frac{5.7}{\bar{k}_E}. \qquad [8]$$

The last term in the right-hand side of the above equation can be neglected because, in biological networks, $\bar{k}_E \gg 5$. Therefore, we obtain again that a good approximation for the ratio between excitatory and inhibitory inputs in the network is given by the two critical points through the equation $m_{EI}/m_E \simeq 1 - \bar{k}_I/\bar{k}_E$. This is the relation we use to describe the experimental data.

1. Papa M, Bundman MC, Greenberger V, Segal M (1995) Morphological analysis of dendritic spine development in primary cultures of hippocampal neurons. *J Neurosci* 15:1–11.
2. Wagenaar DA, Pine J, Potter SM (2006) An extremely rich repertoire of bursting patterns during the development of cortical cultures. *BMC Neurosci* 7:11.
3. Scanziani M, Debanne D, Müller M, Gähwiler BH, Thompson SM (1994) Role of excitatory amino acid and GABAB receptors in the generation of epileptiform activity in disinhibited hippocampal slice cultures. *Neuroscience* 61:823–832.
4. Honore T, *et al.* (1988) Quinoxalinediones: Potent competitive non-NMDA glutamate receptor antagonists. *Science* 241:701–703.
5. Markram H, Tsodyks M (1996) Redistribution of synaptic efficacy between neocortical pyramidal neurons. *Nature* 382:807–810.
6. Keller BU, Konnerth A, Yaari Y (1991) Patch clamp analysis of excitatory synaptic currents in granule cells of rat hippocampus. *J Physiol* 435:275–293.
7. Thomson AM, Deuchars J, West DC (1993) Large, deep layer pyramid-pyramid single axon EPSPs in slices of rat motor cortex display paired pulse and frequency-dependent depression, mediated presynaptically and self-facilitation, mediated postsynaptically. *J Neurophysiol* 70:2354–2369.
8. Crunelli V, Forda S, Kelly JS (1984) The reversal potential of excitatory amino acid action on granule cells of the rat dentate gyrus. *J Physiol* 351:327–342.
9. Kelso SR, Ganong AH, Brown TH (1986) Hebbian synapses in hippocampus. *Proc Natl Acad Sci USA* 83:5326–5330.
10. Kamioka H, *et al.* (1996) Spontaneous periodic synchronized bursting during formation of mature patterns of connections in cortical cultures. *Neurosci Lett* 206:109–112.
11. Breskin I, Soriano J, Moses E, Tlusty T (2006) Percolation in living neural networks. *Phys Rev Lett* 97:188102.

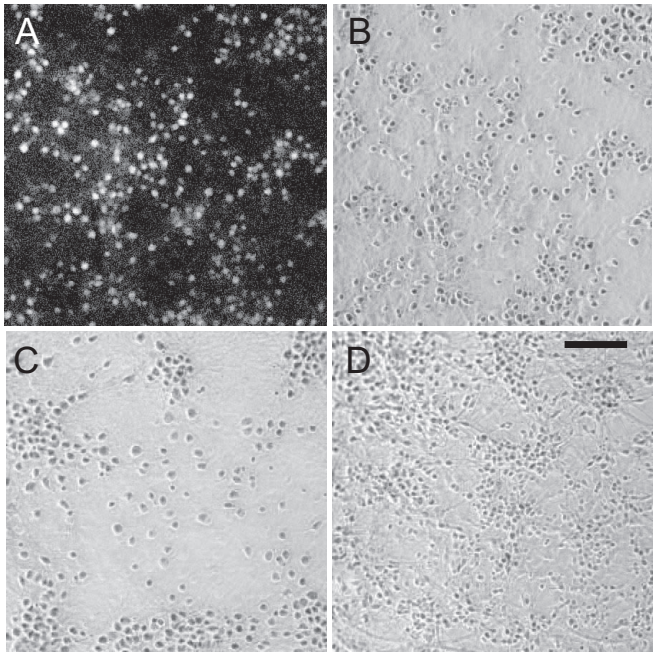

Fig. S1. Microsope images of typical neuronal cultures. (*A* and *B*) Fluorescence and phase contrast images of an E19 hippocampal culture at day *in vitro* (DIV) 16. Bright spots in *A* are neurons that fire in response to the external excitation. (*C* and *D*) Phase contrast images of an E19 cortical culture at DIV 16, and an E17 hippocampal culture at DIV 4. (Scale bar, 100 μm.)

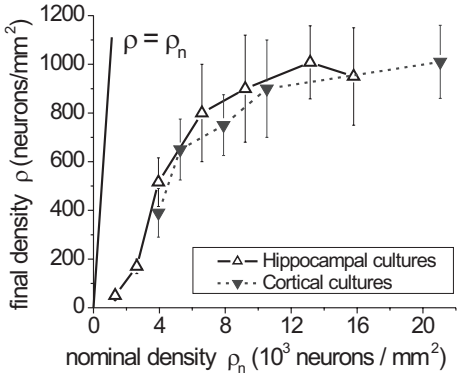

Fig. S2. Final density of the neural culture as a function of the nominal density, for hippocampal and cortical cultures. Each point is an average over 3–7 cultures from different batches. The error bars show the standard deviation.

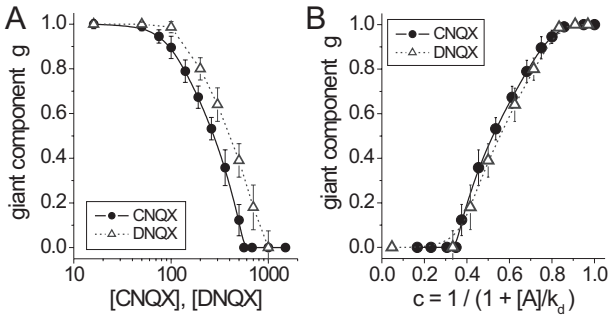

Fig. S3. Determination of the order parameter. (*A*) Size of the giant component for G_{EI} hippocampal cultures studied as a function of the concentration of CNQX (filled circles, average over 16 experiments) and DNQX (open triangles, average over 6 experiments). Lines are a guide for the eye. (*B*) The two curves collapse when the giant component is plotted as a function of $c = 1/(1 + [A]/K_d)$, with $[A]$ the concentration of antagonist (CNQX, $K_d = 300$ nM; or DNQX, $K_d = 500$ nM).

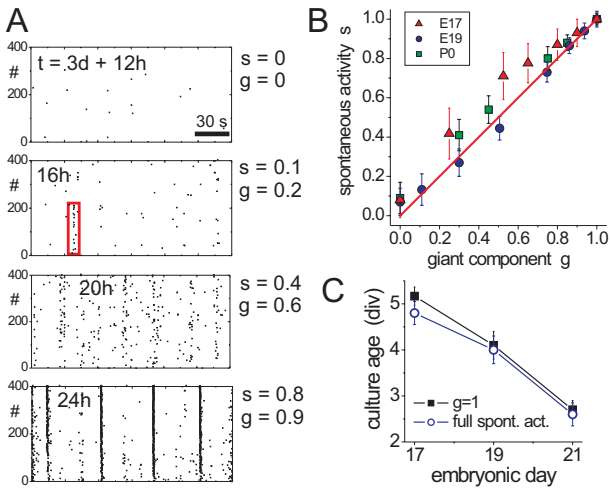

Fig. S4. Spontaneous activity during development. (*A*) Raster plots of spontaneous activity during the formation of the giant component for E19 cultures, measured at 4-h intervals starting at DIV 3.5. Each plot shows the activity of 400 individual neurons along 3 min. The red box outlines the largest fraction of neurons *s* that fired together. (*B*) Largest fraction of neurons in the network that show synchronized spontaneous activity as a function of the size of the giant component, and for E17 (2 experiments), E19 (7 experiments), and P0 (2 experiments) cultures. The line corresponds to slope 1. (*C*) Time at which $g = 1$ (squares) and time of emergence of spontaneous activity extending the entire network (circles) as a function of the embryonic day of the cultures.

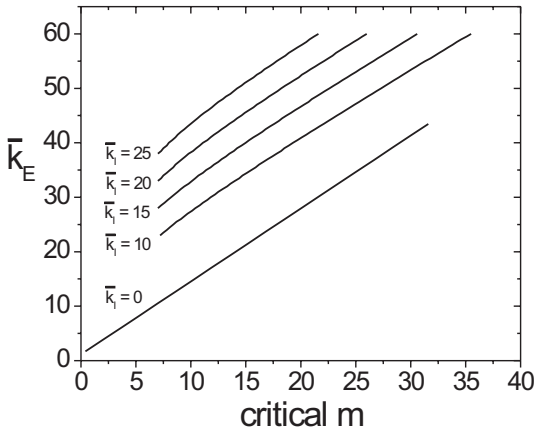

Fig. S5. Dependence of $\bar{k}_E$ on the critical m for a Poisson distribution and for gradually higher amount of inhibition. The curves for $\bar{k}_I > 0$ are cut for low values of m, because they correspond to the regime with $\bar{k}_I < \bar{k}_E$.

Table S1. Range of variation of g_{syn} reported in the literature and corresponding value of $m_0 = V_T/g_{syn}$, with $V_T = 30$ mV

g_{syn} range, mV	m_0	Reference
1.17 ± 0.23	26	Markram *et al.* (5)
1.2 ± 2.8	25	Keller *et al*. (6)
1.67 ± 1.66	18	Thomson *et al.* (7)
5.5 ± 1.1	5	Crunelli *et al*. (8)
6.2 ± 3.8	5	Kelso *et al.* (9)